Real Effect or Artifact of Cloud Cover on Aerosol Optical Thickness?

M-J. Jeong and Z. Li
Department of Meteorology/Earth System Science Interdisciplinary Center
University of Maryland
College Park, Maryland

Introduction

Aerosol measurements over the Atmospheric Radiation Measurement (ARM) Climate Research Facility (ACRF) Southern Great Plains (SGP) site characterize the temporal variability, vertical distribution, and optical properties of aerosols in the region. They were made by the Cimel sunphotometer and multi-filter rotating shadowband radiometer (MFRSR), Raman lidar, in situ Aerosol Profiling (IAP) flights, and the Aerosol Observing System (AOS). The spatial variability of aerosols relies a network of MFRSR at the Central Facility and Extended Facilities, together with satellite remote sensing. The current state-of-the-art satellite-based estimates over land– e.g., MODerate resolution Imaging Scanner (MODIS) aerosol optical thickness (AOT; Kaufman et al. 1997) – still suffer from large uncertainties (±0.05±0.2*AOT; Chu et al. 2002). Contamination due to sub-pixel and/or thin cirrus clouds is believed to be one of the major sources of uncertainties. Retrievals near clouds are discouraged to use, which reduces considerably the amount of useful data. In this regard, cloud is considered as an artifact. However, cloud could have a real impact on AOT by changing humidity, which affects aerosol through the aerosol swelling effect.

As a preliminary study, we first investigate the effects of cloud cover and humidity on the retrievals of AOT from ground-based Cimel sunphotometer measurements, to help us sort out the real influence and artifact. In general, it is difficult to verify and quantify the effects of cloud on satellite retrieval of aerosol quantities. Speculation and warning of cloud contamination have been made whenever there is a correlation between the retrieved AOT and cloud fraction or their spatial variabilities (e.g., Ignatov and Nalli 2002; Jeong and Li 2005), while it has also been argued that aerosol humidification effect (AHE) might be at work. The ample measurements available from ARM over the SGP region may allow us to unravel this complex issue. Our ultimate goals are to (1) evaluate various effects on the retrievals of AOT from both satellite and ground sensors, (2) separate artifact from real effect, and (3) create “clean” aerosol products for studying their direct and indirect effect. We presented some very preliminary findings.

Data

This study employed AOT data from the Cimel sunphotometer of the AErosol RObotic NETwork (AERONET; level 2.0, cloud-screened and quality assured) and cloud mask data from the total sky imager (TSI) measured over the ACRF SGP site (Central Facility) for 2 years between 2003 and 2004.

The AERONET AOT used in this study is the one at 550 nm linearly interpolated from AOT at 500 nm and 675 nm. The profiles for aerosol extinction and relative humidity (RH) from Raman lidar (Goldsmith et al. 1998) are used to compute (aerosol extinction weighted) column mean RH.

Results

Cloud cover from the TSI at the time the AERONET AOT observations was obtained then AERONET AOT was plotted against the cloud cover in Figure 1. It is clearly shown that the AERONET AOT increases with increasing cloud cover. What causes such correlation between AOT and cloud cover? We think several factors may bring such correlation: (1) aerosol humidification or aerosol swelling effects (AHE) along with increasing RH coincident with increasing cloud cover, (2) increasing aerosol concentration due to convergence, (3) increasing number of cloud-processed particles, (4) new particle genesis, (5) cloud contamination in AERONET AOT, and (6) artifact due to cloud detection problems using the TSI.

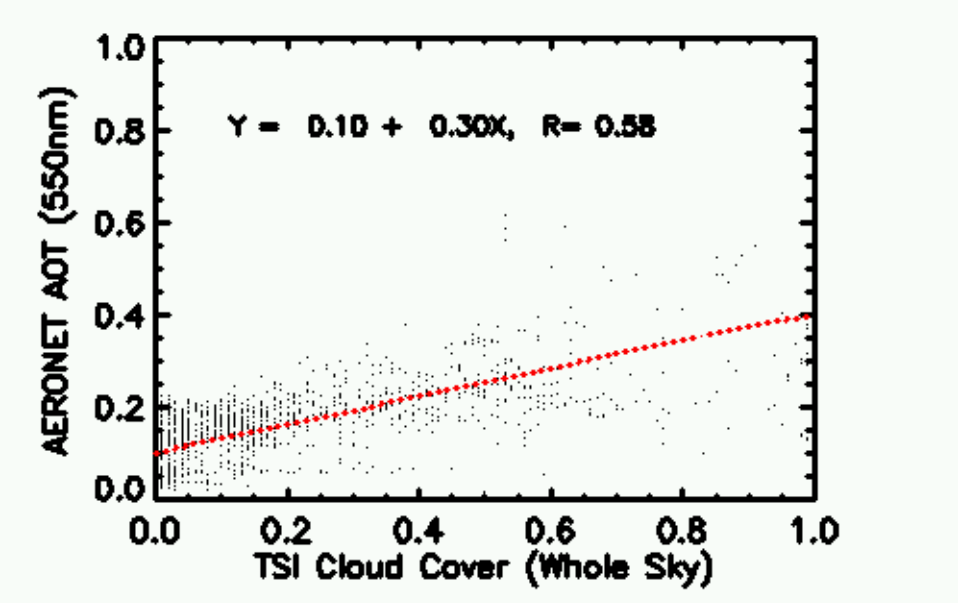

Figure 1. AERONET AOT as a function of cloud cover from the TSI. The red dotted line is the least squared fit line, and R stands for correlation coefficient.

TSI captures images of sky using charge-coupled device (CCD) imager looking down onto a mirror reflecting hemispheric sky, and a shadowband on the mirror blocks the direct sunlight to protect the optics of the imager. The fractional sky cover is determined by examining the relationships between the colors of the acquired image pixels to infer if a pixel represents clear sky, or thin or opaque clouds (Long et al. 2001). It is difficult to discriminate clear sky from clouds around the sun's position because the color relationship near the sun's position is similar to that for clouds (Long et al. 2001). Therefore, it is necessary to check if the correlation shown in Figure 1 is artifact or not. To this purpose, we derive the cloud cover for circum-solar area with various angular distances (A_d) from the sun's position (Figure 2). As provided in Figures 2 and 3, A_d was calculated for all the pixels of a TSI image; then, cloud cover was acquired for the circum-solar areas with increasing the angular radius by 10° from the

sun's position. That is, we compute cloud cover for the circum-solar area within 10°-20° of angular distance, then for the area within 10°-30°, 10°-40°, etc. The results show that the correlations between AERONET AOT and TSI cloud cover exist for all the circum-solar areas (Figure 4). Interestingly, the number of the data points in the bottom-right side of each panel decrease as the circum-solar areas for which cloud cover was computed increase, rendering better correlations (correlation coefficient, R, from 0.33 to 0.58). For easier comparison, AERONET AOT in every other panel in Figure 4 was averaged for the bins of cloud cover with a 0.05 interval and provided in Figure 5. It is evident that AERONET AOT bears a stronger relationship–in terms of both slope and correlation coefficients–with cloud cover as the circum-solar area increases. This result indicates that the correlation may not be an artifact due to problem of TSI cloud mask; otherwise, stiffer slopes would have been found for inner circum-solar areas because enhanced aureole radiation by aerosol scattering would cause more difficulty in cloud discrimination from clear sky. On the other hand, the increasing slopes with increasing circum-solar areas seems reasonable if the effects of cloud cover are related to increasing AHE, convergence, or processed/new particles. These effects would not significantly depend on the local clouds around the sun. Cloud contamination is one effect that may be associated with the local clouds near the sun. The cloud-screening algorithm for AERONET uses temporal variability at various time-scales such that it is known to filter out variable clouds very effectively (Smirnov et al. 2000; Kaufman et al. 2005). Cloud contamination that may exist in AERONET AOT would be due to thin steady clouds (cirrus and some low clouds according to our visual examination). However, the TSI cloud mask often fails to detect such thin clouds; therefore, cloud contamination is not likely the major contributor to the observed correlation between the AERONET AOT and TSI cloud cover.

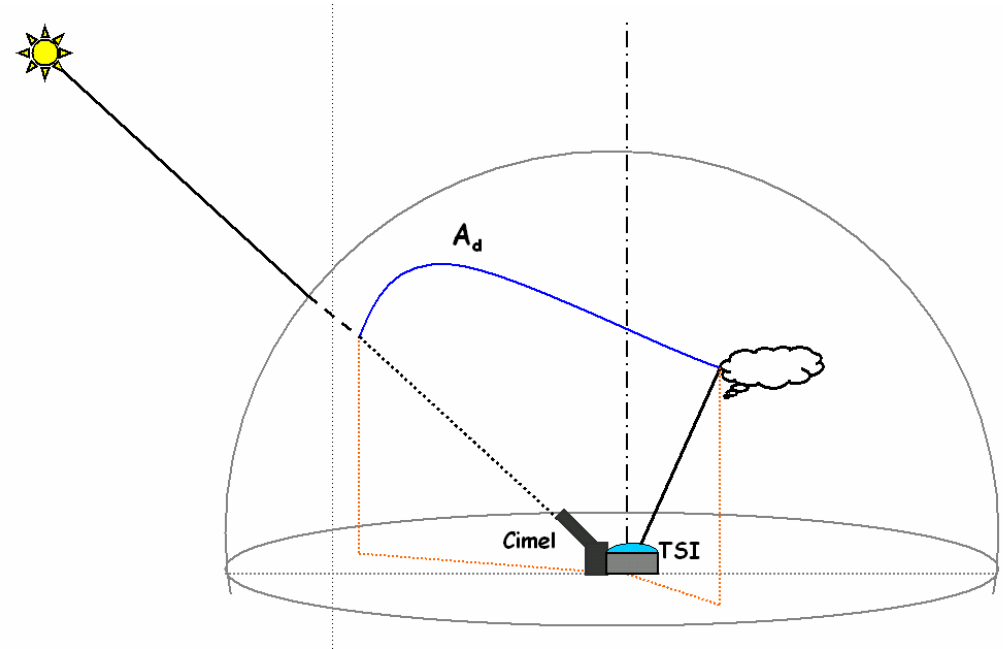

Figure 2. Geometry of observation for the Cimel sun-photometer and for the TSI. A_d stands for an angle between the pixel of the sun's position and any other pixels in a whole sky image taken by the TSI.

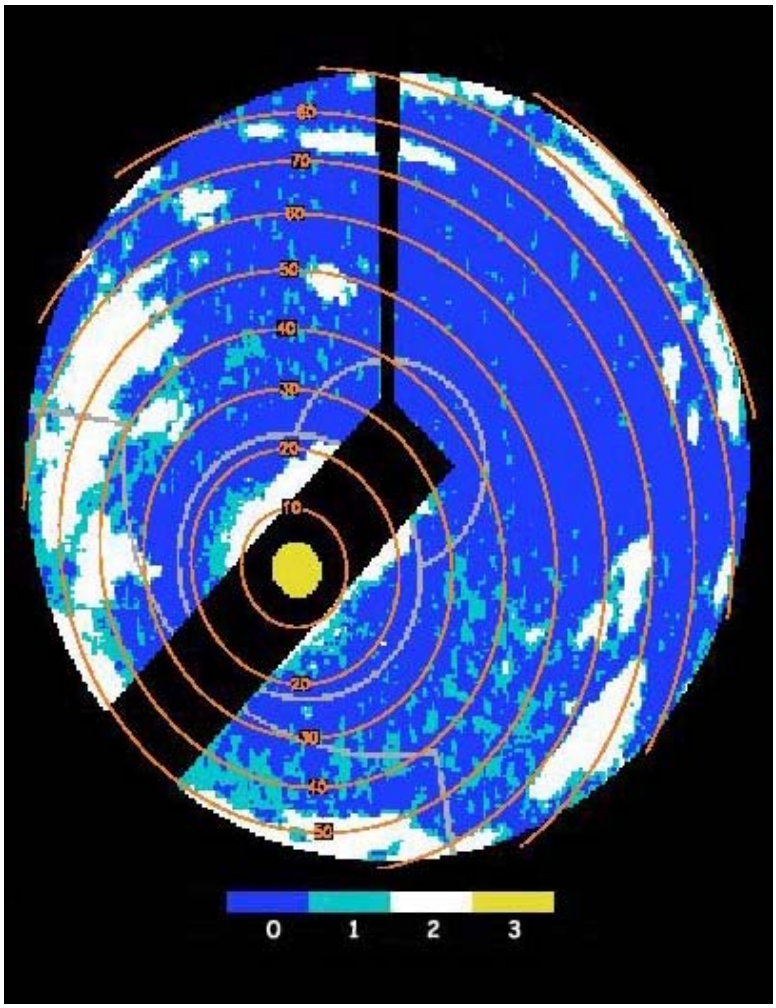

Figure 3. A sample image of cloud mask from TSI. Index 0, 1, 2, and 3 stand for "clear sky," "thin cloud," "opaque cloud," and "location of the sun," respectively. Circum-solar areas for which cloud cover is acquired are presented together with the cloud mask image.

Although Figures 4 and 5 support the idea that the correlation is not an artifact due to the uncertainty in TSI cloud mask, a direct proof is desired. Since the problem of TSI cloud mask happens near the sun's position, we re-compute the cloud cover after the data nearest to the sun's position are removed. In Figure 6, cloud cover for panel (a) was computed for circum-solar area within 10°-50°, panel (b) within 20°-50°, panel (c) within 30°-50°, and panel (d) within 40°-50°. According to our visual examination, TSI cloud masking is rarely affected by intense aureole radiation for angular distance greater than 40° except for large solar zenith angles (e.g., >70°); therefore, we do not expect a significant correlation due to the erroneous TSI cloud mask in panel (d). Therefore, the strongest correlation with the largest slope in panel (d) provided in Figure 6 suggests that the correlation should not be an artifact. Also, small changes in slopes, intercepts, and correlations among the four panels in Figure 6 implies that the problem of TSI cloud masking near the sun's position do not have any significant effect on the statistics regarding the correlation between AOT and cloud cover.

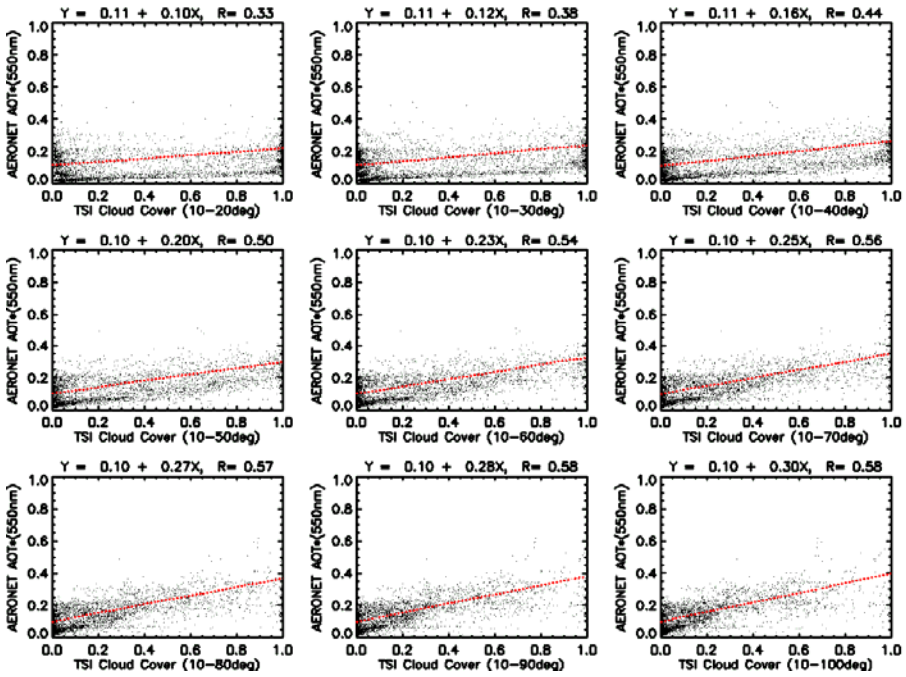

Figure 4. Scatter plots of AERONET AOT as a function of TSI cloud cover for the circum-solar areas within different angular distances from the line of sight to the sun. AERONET AOT shown here is interpolated for the one at 550 nm from AERONET AOTs measured at 500 nm and 670 nm.

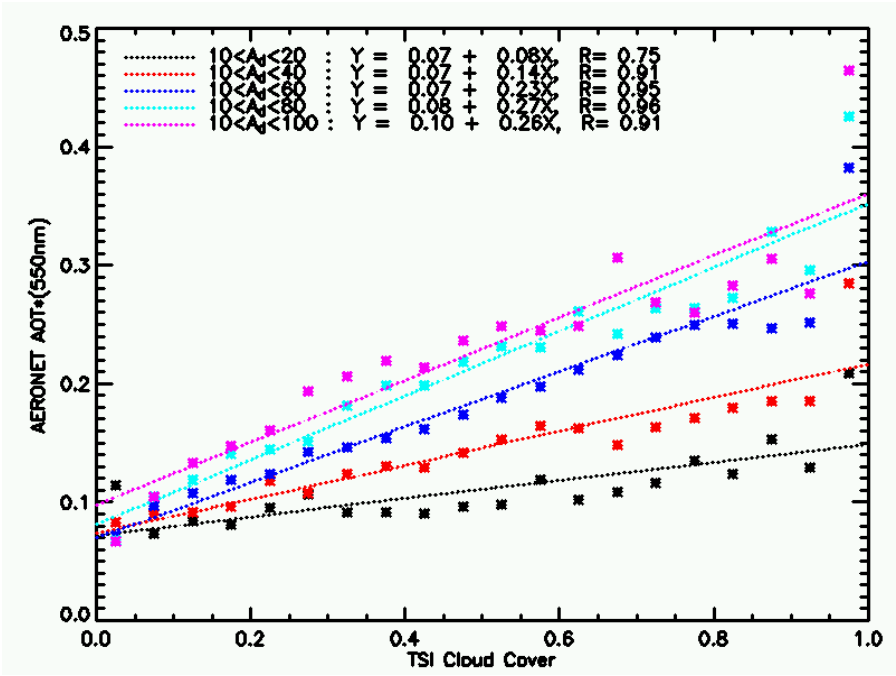

Figure 5. The data shown in Figure 4 were binned according to TSI cloud cover with an interval of 0.05; then AERONET AOT was averaged for each cloud cover bin. Provided here correspond to the data for five panels (every other panel) in Figure 4.

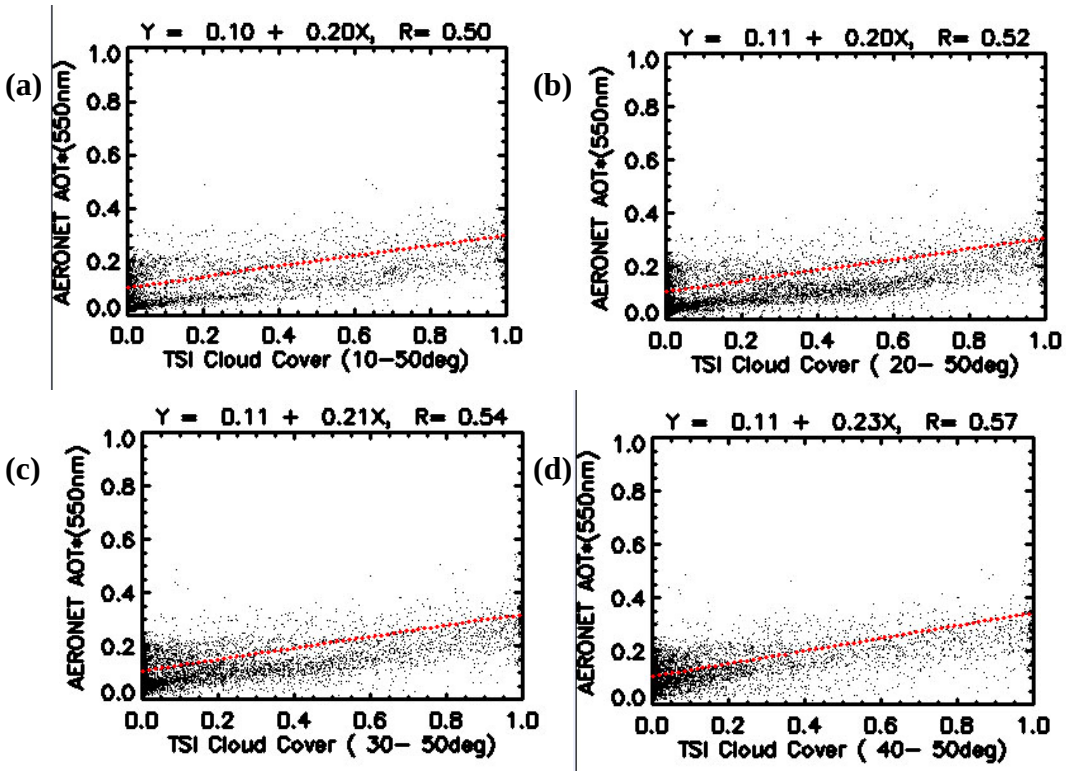

Figure 6. (a) AERONET AOT as function of TSI cloud cover for circum-solar areas with angular distance from the sun's position between 10° and 50°. (b) The same as (a) but with angular distance 20°-50°. (c) The same as (a) but with angular distance 20°-40°. (d) The same as (a) but with angular distance 40°-50°.

Now the remaining possibilities are AHE, convergence, processed particles and new particle genesis along with increasing cloud cover. First, we try to examine the relationship between cloud cover, RH, and AOT. Figure 7 provides AERONET AOT as a function of TSI cloud cover (top) and as a function of aerosol extinction weighted column mean RH, <wRH> (middle), and <wRH> as a function of TSI cloud cover (bottom). Variables in Y-axis are averages over the bins of X-axis with interval of 0.05. <wRH> was calculated using the profiles of RH and aerosol extinction from Raman lidar. It is shown that AERONET AOT is also well correlated to <wRH> as well as cloud cover. The slopes are nearly equal (0.24) and the correlation coefficients, R, are also similar to each other (0.88 and 0.92). However, intercepts are somewhat different (0.12 and 0.04), and interestingly, the regression slope and correlation between <wRH> and cloud cover are very low. It should be noted that the dynamic range of the binned average of <wRH> against TSI cloud cover is confined between 0.4 and 0.7 throughout the cloud cover range between 0 and 1. This result indicates that increasing cloud cover is not necessarily accompanied by increasing column RH. <wRH> and cloud cover seems somewhat independent from each other. Thus, the comparable correlations of the two variables with AOT are likely to be associated with different factors. At this point, we speculate cloud-processed particles (and new particles) may be related to correlation between AOT and cloud cover, while AHE might be linked to the one between AOT and <wRH>. Common contribution of cloud cover and <wRH> may be considered associated with convergence of aerosols along with increasing clouds and water vapor.

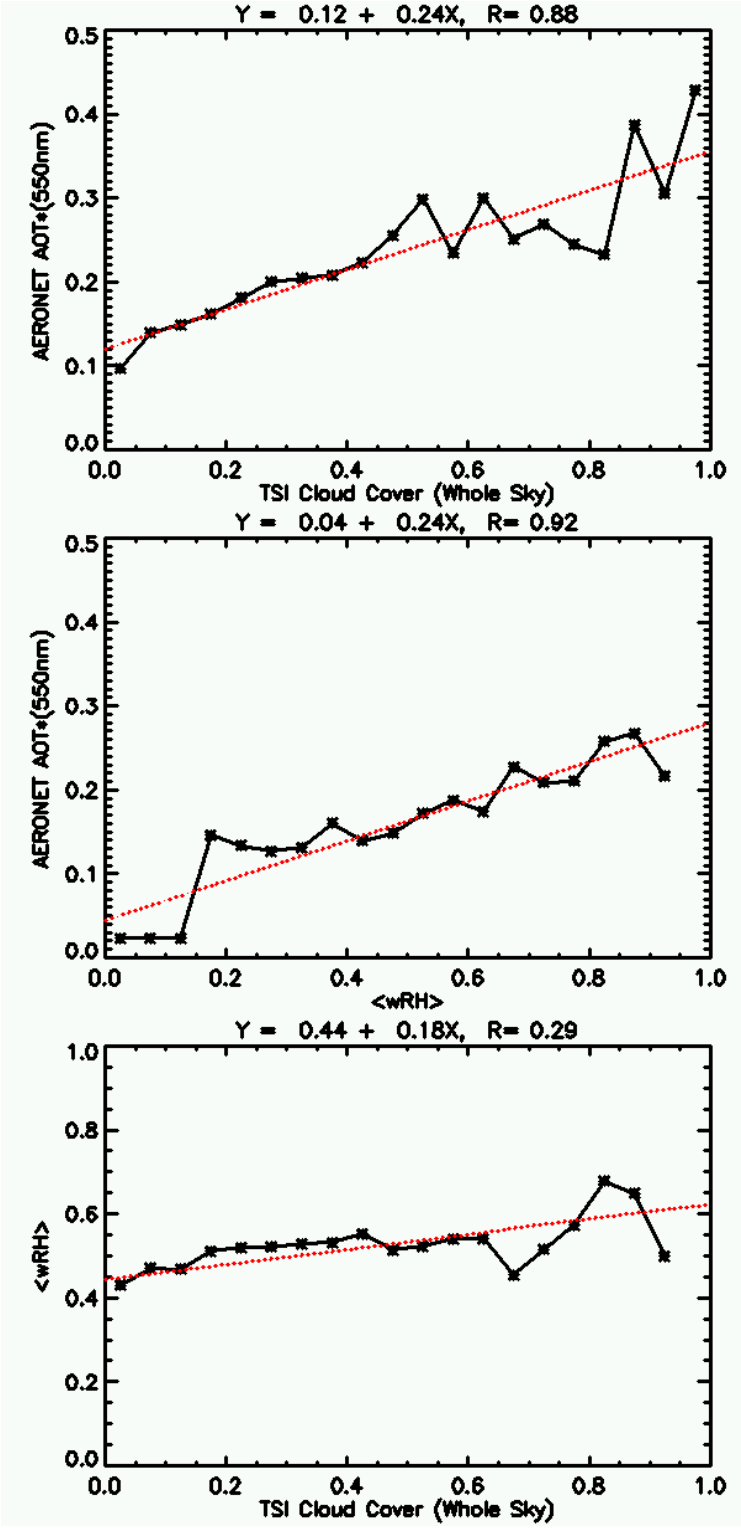

Figure 7. Binned average of AERONET AOT as a function of TSI cloud cover (top), binned average of AERONET AOT as a function of aerosol extinction weighted column mean RH, <wRH> (middle), and binned average of <wRH> as a function of TSI cloud cover (bottom).

Conclusion

We report that AOTs are correlated with cloud cover and it is not simply due to cloud contamination or humidified aerosols but also possibly due to other contributors such as convergence, cloud-processed, or new particles in the presence of clouds. Thus, we propose that more studies on those processes are necessary since it would be very important to find the links between the aerosols and clouds to understand their impacts on the climate of the earth.

Acknowledgement

The data used in this study were obtained from the ARM Program sponsored by the U.S. Department of Energy, Office of Science, Office of Biological and Environmental Research, Climate Change Research Division. We also thank Dr. Rick Wagener and Dr. Brent Holben for their effort in establishing and maintaining the "Cart_Site" and "CART_SITE" for the AERONET. This work is supported by the U.S. DOE ARM program grant DE-FG02-01ER63166 managed by Dr. Wanda Ferrell.

Corresponding Author

Mr. Myeong-Jae Jeong, mjeong@atmos.umd.edu

References

Chu, DA, YK Kaufman, C Ichoku, LA Remer, D Tanré, and BN Holben. 2002. "Validation of MODIS aerosol optical depth retrieval over land." *Geophysical Research Letters* 29(12), doi:10.1029/2001GL013205.

Goldsmith, JEM, FH Blair, SE Bisson, and DD Turner. 1998. "Turnkey Raman lidar for profiling atmospheric water vapor, clouds, and aerosols." *Applied Options* 37, 4979-4990.

Ignatov, A and NR Nalli. 2002. "Aerosol retrievals from multi-year multi-satellite AVHR Pathfinder Atmosphere (PATMOS) dataset for correcting remotely sensed sea surface temperatures." *Journal of Atmospheric and Oceanic Technology* 19, 1986-2008.

Jeong, M.-J and Z Li. 2005. "Quality, compatibility and synergy analyses of global aerosol products derived from the advanced very high resolution radiometer and Total Ozone Mapping Spectrometer." *Journal of Geophysical Research* 110, D10S08, doi:10.1029/2004JD004647.

Kaufman, YJ, D Tanré, LA Remer, EF Vermote, A Chu, and BN Holben. 1997. "Operational remote sensing of tropospheric aerosol over land from EOS moderate resolution imaging spectroradiometer." *Journal of Geophysical Research* 102(D14), 17051-17067.

Kaufman, YJ, LA Remer, D Tanré, R-R Li, R Kleidman, S Mattoo, R Levy, T Eck, BN Holben, C Ichoku, V Martins, and I Koren. 2005. "A critical examination of the residual cloud contamination and diurnal sampling effects on MODIS estimates of aerosol over ocean." manuscript submitted.

Long, CN, DW Slater, and T Tooman. 2001. Total Sky Imager Model 880 status and testing results. ARM/TR-006, 36 pp.

Smirnov, A, BN Holben, TF Eck, O Dubovik, and I Slutsker. 2000. "Cloud-screening and quality control algorithms for the AERONET database." *Remote Sensing Environment* 73, 337-349.

Turner, DD and JEM Goldsmith. 1999. "Twenty-four-hour Raman lidar measurements during the Atmospheric Radiation Measurement program's 1996 and 1997 water vapor intensive observation periods." *Journal of Atmospheric Oceanic Technology* 16, 1062-1076.

Turner, DD, RA Ferrare, and LA Brasseur. 2001. "Average aerosol extinction and water vapor profiles over the Southern Great Plains." *Geophysical Research Letters* 28(23), 4441-4444.